Check for updates

ECOLOGY

Kelp forest loss and emergence of turf algae reshapes energy flow to predators in a rapidly warming ecosystem

Dara S. Yiu[1,2]*, Emma A. Elliott Smith[3], Shane P. Farrell[1,2], Douglas B. Rasher[1]

Copyright © 2025 The Authors, some rights reserved; exclusive licensee American Association for the Advancement of Science. No claim to original U.S. Government Works. Distributed under a Creative Commons Attribution NonCommercial License 4.0 (CC BY-NC).

Climate change is decimating habitat-forming species in ecosystems around the world. Yet, the impacts of habitat loss on the energetics of the wider food web remain uncertain for many iconic ecosystems, including cold-water kelp forests. Here, we assessed how the loss of kelp forests and the subsequent proliferation of low-lying turf algae in the Gulf of Maine have altered the trophic niches of, and energy acquired by, predatory reef fishes. Bulk tissue $\delta^{13}C$ and $\delta^{15}N$ analysis showed that fishes in kelp forests had larger trophic niches and greater interspecific niche separation than fishes on turf reefs. Moreover, $\delta^{13}C$ analysis of essential amino acids revealed that kelp-derived energy accounted for most of the energy used by kelp forest fishes (> 50% on average), whereas fishes on turf reefs compensated for kelp decline via greater reliance on a phytoplankton-based energy channel. Therefore, ecosystem state shifts to turf algae—now a global phenomenon—may have far-reaching impacts on food web energetics and resilience.

INTRODUCTION

The creation and flow of energy in nature underpin how ecosystems function and influence their biodiversity, productivity, and resilience (*1*). Large-scale disturbances that cause habitat-forming species to decline can thus alter the flux of energy in ecosystems either by removing key energy sources or by altering the conduits of energy within a food web via changes in predator-prey interactions (*2*). For example, transforming terrestrial forests into crop monocultures or deforested land restructures soil communities, redefines the relative importance of different carbon sources to stream fauna, and reduces the niche breadth of bird trophic guilds (*3*–*5*). Likewise, on tropical coral reefs, the loss of habitat-forming corals alters fish assemblages and associated predator-prey interactions, resulting in altered energy dynamics (*6*, *7*). Yet, our understanding of how habitat-formers shape energy flow in other coastal food webs is limited. For example, while kelp forests define much of Earth's temperate coastline (*8*) and house myriad animal species (*9*, *10*), the degree to which kelp-derived energy supports predators—and the corresponding impacts of kelp loss on energy flow—remains unknown for most kelp forest ecosystems (*11*).

As foundation species (*12*), kelps may influence coastal food webs by providing habitat or food resources. The underwater structures created by these large, canopy-forming brown macroalgae provide refuge for animals, including small invertebrates, which, in turn, affect the distribution and foraging behaviors of vertebrate predators (*13*–*15*). Further, kelps serve as a source of benthic (reef-based) energy, therein providing carbon and essential nutrients that support the biomass of grazers, filter feeders, and secondary consumers, such as fishes (*16*–*18*). Hence, the loss of kelp can reshape food web dynamics when this key source of energy is reduced or extirpated. For instance, when overgrazing by herbivores denudes the reef of seaweed [e.g., "urchin barrens" in the North Pacific (*19*)], the loss of kelp not only alters fish community structure and faunal diversity (*20*) but also reshapes consumer niches and energy flow within coastal food webs (*17*, *21*, *22*).

Recently, an alternate ecosystem state shift has emerged in areas of rapid ocean warming, where kelp forests are giving way to reefs dominated by small red "turf" algae (*23*). This shift markedly alters the functional characteristics of the macroalgae that define these coastal ecosystems; it shrinks the size of biotic habitat from canopy heights of meters to centimeters (*24*, *25*) and reduces the living biomass of macroalgae on the reef from kilograms to grams per square meter (*26*). These changes may also alter the primary production pathways that underlie the structure of local food webs. For instance, in western Australia, where a kelp-to-turf state shift coincided with the arrival of tropical turf-eating herbivorous fishes (*27*), food webs were redefined around the emerging importance of red turf algae (*28*). However, transitions from large, canopy-forming species to low-lying turf algae are now occurring in many other marine ecoregions, including southern Australia (*29*), Japan (*25*), the Mediterranean Sea (*30*), and the North Atlantic (*31*, *32*). In high latitude regions, kelp-to-turf transitions are less likely to co-occur with an influx of tropical species [e.g., (*33*)]. Instead, changes may occur through (i) redefining species interactions and (ii) reshaping the diversity of "energy channels" [i.e., pathways by which distinct basal resources are transferred through trophic levels (*2*, *34*)] that are available in the ecosystem. Therefore, it is critical that we assess how animals adapt and alter their trophic interactions and energy acquisition in the face of kelp loss and turf proliferation.

Here, we explored the effects of a kelp-to-turf state shift on the trophic ecology of two dominant predatory fishes (generalist secondary consumers) in the Gulf of Maine, a region of the Northwest Atlantic where kelp forests historically spanned the rocky coastline (*35*). Since the turn of the 21st century, ocean warming has driven rapid kelp forest decline, with the most severe declines occurring in the warmest portions of the Maine coastal current. In southwestern Maine, forests have widely collapsed (~80% loss in kelp cover from 2004 to 2018), and these reefs have subsequently become dominated by turf algae (*24*, *32*). In contrast, kelp forests continue to persist in

[1]Bigelow Laboratory for Ocean Sciences, East Boothbay, ME 04544, USA. [2]Darling Marine Center, University of Maine, Walpole, ME 04563, USA. [3]Department of Biology and Center for Stable Isotopes, University of New Mexico, Albuquerque, NM 87131, USA.
*Corresponding author. Email: dsy.371@gmail.com

Downloaded from https://www.science.org at National University of Ireland, Galway on August 20, 2025

the cooler, northeastern reaches of the Maine coast (*32*). Hence, this system has become a "natural laboratory" for assessing the impacts of a kelp-to-turf state shift on energy flow to predators.

We first surveyed macroalgae and fish assemblages along the Maine coast to characterize the abundance of basal energy resources available to common predatory fishes in kelp forests (northeast Maine), in transitioning mixed-state reefs (central Maine), and on turf-dominated reefs (southwest Maine; Fig. 1). Across these habitats, we then assessed the trophic niche breadth of, and niche partitioning between, the two most abundant predatory fish species in the ecosystem using bulk muscle tissue carbon and nitrogen stable isotope analyses ($\delta^{13}C$ and $\delta^{15}N$; Fig. 2). Last, by analyzing carbon stable isotope ratios of essential amino acids ($\delta^{13}C_{EAA}$; Fig. 3), we quantified the degree to which predatory fishes use kelp-derived carbon as energy, and how their energy use changes as kelp forests are lost and replaced by red turf algae (Fig. 4).

RESULTS

Macroalgae and fish assemblages along Maine's coast

We surveyed all macroalgae (canopy-forming kelps and the smaller, understory seaweeds residing under the canopy, including foliose, bladed, and filamentous species) on subtidal rocky reefs across four subregions of Maine. We observed a stark contrast between kelp-dominated reefs in the northeast and turf-dominated reefs in the southwest (Fig. 1). In northeast Maine, kelp forests were mostly comprised of *Laminaria digitata* and *Saccharina latissima*, and kelp biomass was high (Downeast: mean 4.6 kg ± 0.7 SE kelp/m^2). As in

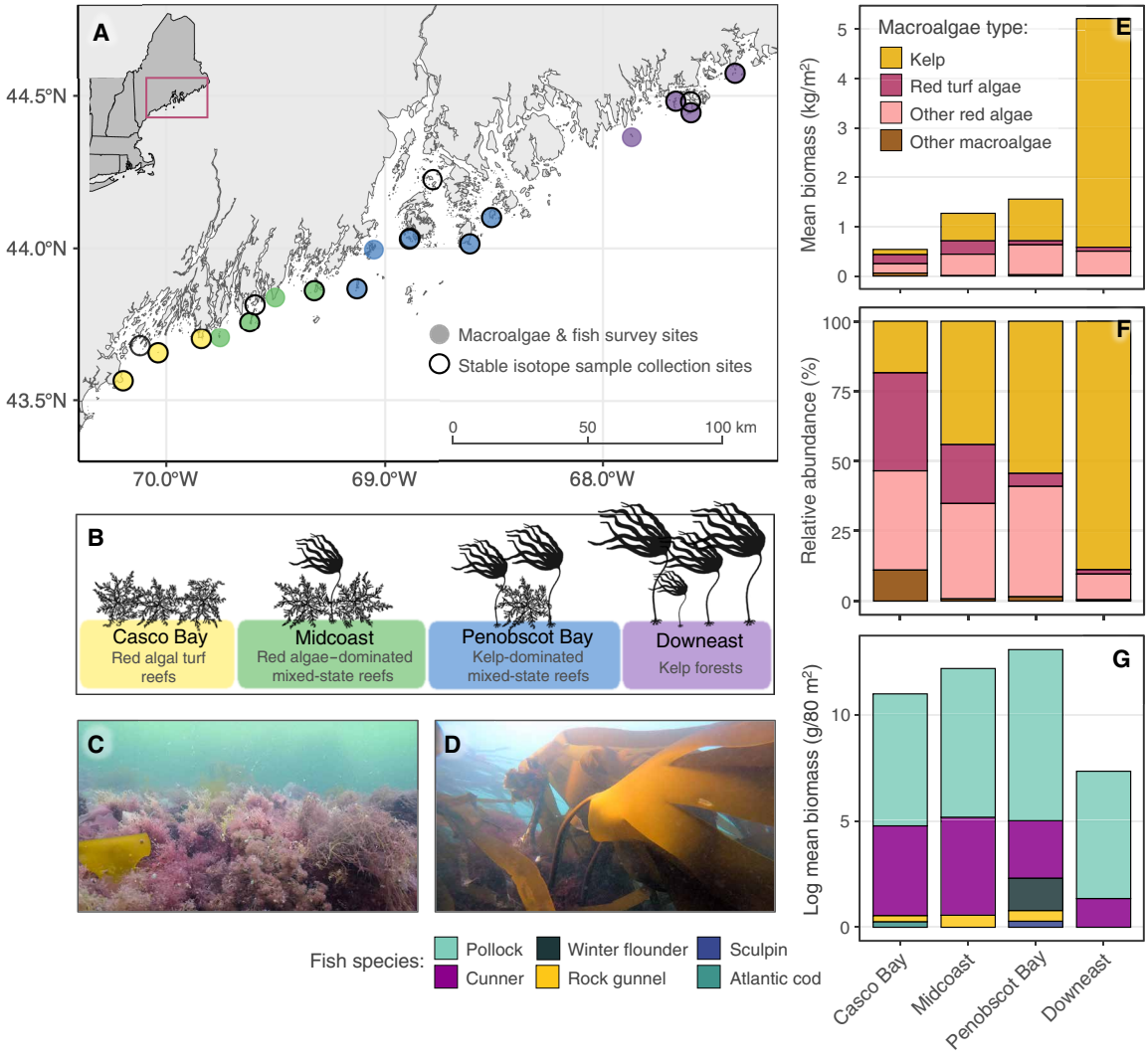


Fig. 1. Macroalgae and fish assemblages across a coastal kelp-to-turf gradient. (**A**) Study sites in four subregions of the coast of Maine, where macroalgae and fish surveys took place in the summers of 2021 and/or 2022 (colored dots) and where samples were collected for stable isotope analysis (dots with black outlines). The Maine state polygon feature was accessed from the Maine GeoLibrary Data Catalog at www.maine.gov/geolib/index.html. These study sites were historically kelp dominated but now span (**B**) a gradient in habitat condition, as reefs in the warmer, southwestern subregions have transitioned to (**C**) turf reefs, while (**D**) kelp forests remain in the northeast. (**E**) Mean biomass of macroalgae (kilograms per square meter), (**F**) relative abundance of macroalgae, and (**G**) composition of fish assemblages (mean biomass of each taxon in grams per 80 m^2, log+1 transformed) in each subregion. "Other red algae" are foliose, cylindrical, and corticated rhodophytes that are not "turf algae" (i.e., filamentous or uniseriate species). "Other macroalgae" include nonkelp ochrophytes (e.g., *Desmarestia* and *Ectocarpus*) and chlorophytes (e.g., *Ulva* and *Chaetomorpha*).

Downloaded from https://www.science.org at National University of Ireland, Galway on August 20, 2025

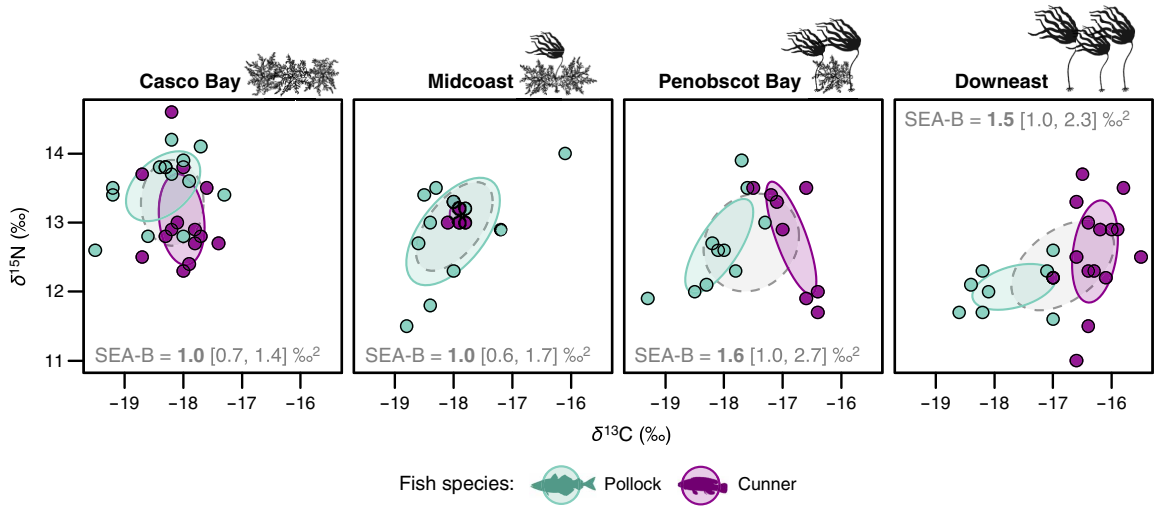


Fig. 2. Predatory fish isotopic niches. Carbon and nitrogen stable isotope (δ^{13}C and δ^{15}N) values (dots) and isotopic niche areas (ellipses) for pollock (turquoise; $n = 10$ to 14 per subregion) and cunner (magenta; $n = 5$ to 15 per subregion). Gray dashed ellipses show the isotopic ellipse areas for all sampled fishes in a given subregion, and gray texts denote those SEA-B modes and 95% credible intervals. All ellipses encompass 40% of points for their respective group.

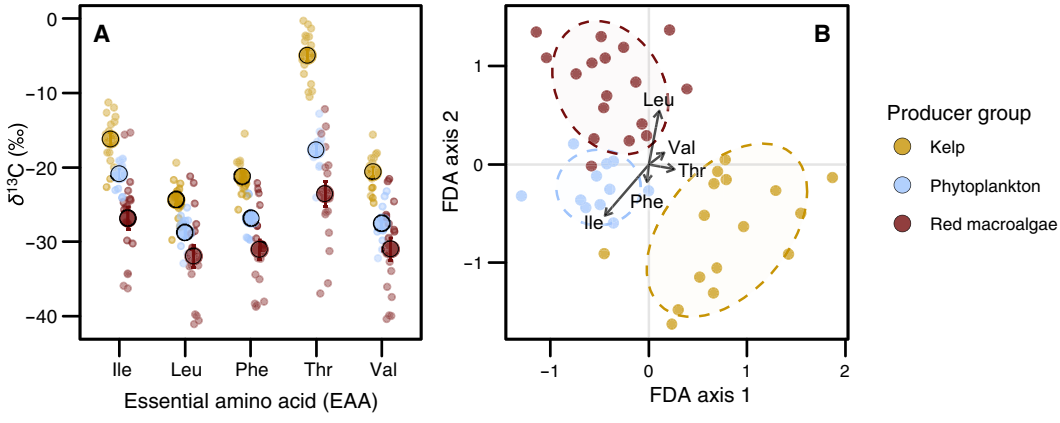


Fig. 3. Carbon stable isotope values of EAAs ($\delta^{13}C_{EAA}$) as primary producer fingerprints. (**A**) Measured $\delta^{13}C_{EAA}$ values of individual kelp (gold), phytoplankton (blue), and red macroalgae (red) samples (small dots) and group means (large dots; ± SE). Individual $\delta^{13}C_{EAA}$ values were used as predictors in an FDA classification model (93.2% accurate reclassification). (**B**) The FDA biplot shows separation between producer samples (dots) along the two discriminant axes. Ellipses encompass 75% of their respective group data. The direction and magnitude of the contribution of each EAA for differentiating producer groups in the FDA model are shown with vectors (scaled 2×). EAAs are abbreviated following convention: isoleucine (Ile), leucine (Leu), phenylalanine (Phe), threonine (Thr), and valine (Val). Colors denote primary producer group.

most kelp forests, red macroalgae were abundant beneath the kelp canopy but contributed proportionally little to the overall macroalgae biomass (Fig. 1).

Conversely, southwestern reefs harbored low macroalgae biomass in general and especially low biomass of kelp (Casco Bay: mean 0.1 kg ± 0.1 SE kelp/m^2). Here, red macroalgae comprised 71% of the total macroalgae biomass, and red turf algae (i.e., those species of red algae with filamentous or uniseriate morphologies that characterize turf reefs) alone made up 35% of biomass. The subregions in central Maine (Midcoast and Penobscot Bay) harbored reefs where kelp was in decline, but the state shift to turf dominance was in various stages of progression (Fig. 1). Consequently, the diversity and amount of macroalgae that could serve as energy to food webs varied significantly across the coast—along a continuum from kelp forests to turf reefs [Jonckheere-Terpstra (JT) trend test, $P < 0.05$; Fig. 1 and table S1].

From visual surveys, we determined that roving fish assemblages—in both kelp forests and turf reefs—were dominated by cunner, *Tautogolabrus adspersus* (family Labridae), and juvenile pollock, *Pollachius virens* (family Gadidae) (Fig. 1G). These species together comprised ~99% of total roving fish biomass. Variation in total fish biomass did not follow a trend (JT, $P > 0.05$) between Casco Bay (563 g/80 m^2 ± 277 SE), Midcoast (1200 g/80 m^2 ± 432 SE), Penobscot Bay (3151 g/80 m^2 ± 874 SE), and Downeast (404 g/80 m^2 ± 225 SE) subregions. These simplified fish assemblages are partly the result of severe overfishing, which, over past centuries, reduced fish abundance and diversity in the Gulf of Maine (*35*, *36*). However, labrids and gadids are common in kelp forests with subsurface canopies around the world [gadids in Northern Hemisphere and labrids in both hemispheres (*33*, *37*)]. Hence, the Gulf of Maine is a tractable ecosystem for studying food web responses to a state shift, and

Downloaded from https://www.science.org at National University of Ireland, Galway on August 20, 2025

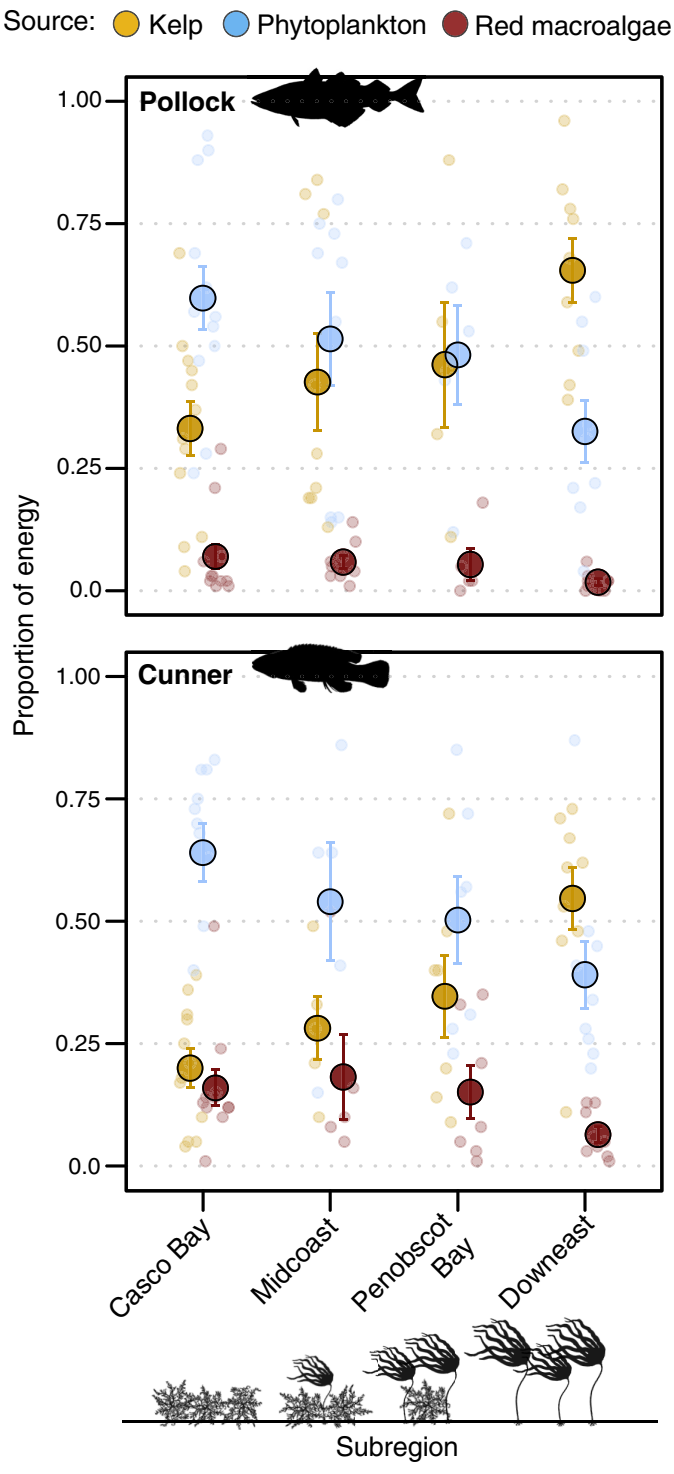


Fig. 4. Energy channel contributions to reef fishes. Proportion of energy that generalist predators (cunner and pollock) acquired from each of three energy channels: kelp-based (gold), phytoplankton-based (blue), and red macroalgae–based channels (red). Fishes were sampled in subregions spanning from kelp forests (Downeast) to mixed-state reefs (Penobscot Bay and Midcoast) to turf reefs (Casco Bay). Proportions of energy that individual fish derived from producers (small dots) were determined by classifying fish $\delta^{13}C_{EAA}$ values in 10,000 bootstrap iterations of an FDA model (Fig. 3B). Large dots are the mean (± SE) contribution from each energy channel per subregion.

the species on which we focused (cunner and pollock) are emblematic of common predators in kelp forests.

Both of these species have generalist diets that are highly variable but often include small crustaceans (amphipods, isopods, and crabs), mollusks (snails and mussels), annelid worms, and fishes. Juvenile pollock are highly mobile predators that can easily move and feed throughout the water column; hence, in addition to the aforementioned prey, they have been reported to eat copepods, mysids, euphausiids, and benthic macroalgae (*38*–*40*). By contrast, cunner have more restricted home ranges and are benthic oriented as adults, where they reportedly forage on a variety of additional benthic prey including sea urchins, barnacles, and encrusting invertebrates (*40*–*42*). Thus, while both species are generalists, their niches may differ in some regards.

Characterizing predatory fish ecology: Isotopic niche area and overlap

For primary producers, differences in bulk tissue carbon ($\delta^{13}C$) and nitrogen ($\delta^{15}N$) stable isotope values reflect variation in photosynthetic strategies, carbon acquisition modes, and inorganic nutrient pools (*43*, *44*). The isotopic composition of animal tissues is similarly affected by their resource use, trophic position, and physiological processes (*45*). Thus, we measured $\delta^{13}C$ and $\delta^{15}N$ of local primary producers, primary consumers, and secondary consumers and assessed isotopic variation within and among subregions (Supplementary Text, figs. S1 to S3, and table S2). We used consumer isotopic niches as proxies for trophic niches (*45*) and henceforth use these terms interchangeably.

Niche breadth of predatory fishes

Collectively, the two dominant reef fishes in Maine (cunner and pollock) had varying isotopic niche sizes in kelp forests, mixed-state reefs, and turf-dominated reefs (Fig. 2). On the basis of Bayesian standard ellipse areas [SEA-B; reported here with 95% credible intervals (*46*)], kelp forest fishes had larger isotopic niches (SEA-B of Downeast fish: 1.5 [1.0, 2.3] ‰^{2}) than fishes from turf-dominated reefs (SEA-B of Casco Bay fish: 1.0 [0.7, 1.4] ‰^{2}). Fishes from the kelp-dominated, mixed-state region (Penobscot Bay) had the largest isotopic niche (SEA-B: 1.6 [1.0, 2.7] ‰^{2}).

Niche overlap among species

Cunner and pollock also had isotopic niches with varying degrees of interspecific overlap. In subregions with kelp forests (Downeast) and kelp-dominated, mixed-state reefs (Penobscot Bay), cunner and pollock had distinct, nonoverlapping isotopic niches (i.e., no overlap in 40%-level ellipses). Conversely, in southwestern subregions dominated by red macroalgae (Midcoast and Casco Bay), niches of the two species strongly overlapped (Fig. 2).

$\delta^{13}C$ and $\delta^{15}N$ values

In addition, fish muscle $\delta^{13}C$ and $\delta^{15}N$ values varied significantly by habitat (Supplementary Text and fig. S3). On kelp-dominated reefs (Downeast and Penobscot Bay), cunner $\delta^{13}C$ values were significantly higher than those of pollock [Kruskal-Wallis rank sum test (KW), $P < 0.05$], while on turf-dominated reefs (Midcoast and Casco Bay), cunner and pollock $\delta^{13}C$ values were indistinct (KW, $P > 0.05$; Fig. 2 and table S3). Fish $\delta^{15}N$ values were also significantly different on kelp-dominated (Downeast) versus turf-dominated (Casco Bay) reefs (KW, $P < 0.05$) but not on mixed-state reefs (Midcoast and Penobscot Bay; KW, $P > 0.05$). Cunner in kelp forests (Downeast) had significantly higher $\delta^{15}N$ values than pollock, whereas on turf-dominated reefs (Casco Bay), the inverse was observed (Fig. 2 and table S3).

Downloaded from https://www.science.org at National University of Ireland, Galway on August 20, 2025

Differences in the relative values of $\delta^{13}C$ and $\delta^{15}N$ for reef fishes across subregions were not a result of size variation and suggest that their predator-prey interactions are different on kelp-dominated versus turf-dominated reefs (figs. S3 and S4).

Energy flow from primary producers to predatory fishes

To understand the role of kelp as a basal energy resource to fishes and how the transfer of producer-derived organic matter to consumers (hereafter, energy flow) changes with kelp forest loss, we quantified the contribution of kelps, red macroalgae (including bladed, foliose, and filamentous turf species), and pelagic phytoplankton to fish muscle tissue via carbon stable isotope analysis of individual essential amino acids ($\delta^{13}C_{EAA}$). While bulk tissue $\delta^{13}C$ values of consumers broadly reflect the resources they have assimilated, these data often cannot provide the resolution needed to quantify the proportional contribution of multiple producer groups to consumer biomass due to substantial spatiotemporal variation in $\delta^{13}C$ values of producers (*47*) and variability in isotopic fractionations associated with trophic transfer within consumers (*48*).

Isotopic analysis of individual compounds within tissues offers many improvements on these issues (*49*). Amino acids are a major conduit of energy flow in food webs, accounting for roughly half of the total carbon in most organisms (*50*). In particular, essential amino acids (EAAs) are critical molecular constituents of proteins that most animals cannot synthesize de novo and must route directly from diet (or gut microbial communities); thus, $\delta^{13}C_{EAA}$ are minimally altered by trophic transfer and act as biomarkers of energy flow through multiple trophic levels (*49*, *51*). Furthermore, $\delta^{13}C_{EAA}$ of nearshore marine primary producers varies among taxonomic groups and appears to be conserved across broad spatiotemporal scales, thus serving as a "fingerprint" that can be used to quantify the contribution of carbon from distinct primary producer groups to consumers across multiple trophic levels (*52*, *53*).

$\delta^{13}C_{EAA}$ fingerprinting

We identified kelp, red macroalgae, and phytoplankton as the major primary producer groups comprising the dominant potential energy channels in the Gulf of Maine (Fig. 1). From samples collected locally in all subregions, we found that each group had distinct $\delta^{13}C_{EAA}$ fingerprints [sensu Larsen *et al.* (*50*); Fig. 3]. A flexible discriminant analysis (FDA) using $\delta^{13}C_{EAA}$ values from five EAAs [isoleucine (Ile), leucine (Leu), phenylalanine (Phe), threonine (Thr), and valine (Val)] as model predictors clearly deciphered each producer group (93.2% reclassification success; Fig. 3B). We thus analyzed energy channel importance to consumers using this FDA model (with 10,000 bootstrap iterations; see Materials and Methods) trained on Gulf of Maine primary producers.

Energy channel use by predatory fishes

We used the FDA to predict the probability that EAAs in fish muscle tissues was derived from kelp versus phytoplankton versus red macroalgae and used these probabilities as estimates of proportional energy contributions [see Elliott Smith *et al.* (*18*)]. From these model predictions, we determined that predatory fishes in kelp forests (Downeast) used kelp-derived energy to a high degree—on average, 60.1% (± 4.6 SE) of their energy was derived from kelp (Fig. 4 and table S4). This finding reveals that kelps with subsurface canopies support an energy channel that is heavily used by forest-associated fishes and, by extension, lower trophic levels in the ecosystem.

In contrast, in subregions where kelp forests have collapsed, the proportion of kelp-derived energy acquired by fishes was notably lower (JT, $P < 0.05$ for both species). Specifically, the kelp-based energy channel was less than half as important for supporting fish biomass on turf reefs as it was in kelp forests (kelp-derived energy in Casco Bay fishes: 26.9% ± 3.6 SE). On reefs dominated by red macroalgae, fishes compensated for this loss of kelp-derived energy by acquiring a large portion of their energy via a pelagic, phytoplankton-based energy channel (JT, $P < 0.05$; Fig. 4 and table S4). Red macroalgae did not provide a notable source of energy to fishes on southwestern reefs, despite that red macroalgae have come to dominate in these locales (red macroalgae–derived energy in Casco Bay fishes: 11.3% ± 2.6 SE). Nonetheless, the contribution of red macroalgae–derived energy to fishes was statistically greater for fishes on turf-dominated versus kelp-dominated reefs (JT, $P < 0.05$).

DISCUSSION

Foundation species are those that define an ecosystem's physical habitat and therefore underpin their community dynamics (*12*). Despite kelp forests and turf reefs both being dominated by macroalgae, they have vastly different physical attributes and modes of primary production. Kelps form large, upright structures with vertical and interstitial spaces that offer refuge and foraging opportunities to fish (*10*). Red turf algae, on the other hand, are a consortium of fast-growing species that form carpet-like mats that are low-lying (1 to 10 cm tall) and highly complex, but only at small scales, owing to their filamentous nature (*24*). Kelp-to-turf state shifts have occurred around the world in recent decades (*23*, *25*), yet the implications of this shift for the provisioning and flow of energy on temperate reefs are not yet clear. Our findings show that predatory fishes within kelp forests in the Gulf of Maine derive most of their energy from kelp. Conversely, a kelp-to-turf state shift across the southern extent of this region changed predators' reliance on basal energy sources, from predominantly benthic to pelagic energy. These results highlight that subsurface canopy kelps—which account for two-thirds of global kelp forest distribution—are a key source of energy to ecologically important predators.

A kelp-to-turf state shift alters predatory fish niche partitioning

Kelp forests are renowned for the massive vertical structures they create on coastal reefs, which regulate species diversity and predator-prey interactions (*14*, *22*). Yet, while turf-dominated reefs lack the large vertical structures afforded by kelp forests, red turf algae do have interstitial spaces that harbor many small benthic invertebrates (*24*). Turf reefs contrast sharply with urchin barrens, where predator loss allows herbivorous sea urchins to strip reefs bare, leaving them devoid of macroalgae. As a result, the shift from kelp dominance to turf dominance represents a fundamentally different ecological transition, raising the question of whether turf-dominated reefs can sustain trophic interactions and niche availability for predatory fishes.

By comparing the bulk carbon and nitrogen stable isotopic values of predatory fishes from kelp-dominated and turf-dominated reefs, we observed that the ecological niche breadth of the fish assemblage was largest on kelp-dominated reefs and contracted in subregions where kelp forests have been replaced by turf algae (Fig. 2). We also found that kelp forests may contribute to structuring trophic interactions and niche partitioning among predatory reef fishes, with the two dominant fish species (pollock and cunner) occupying distinct and nonoverlapping niches in forested subregions versus convergent

Downloaded from https://www.science.org at National University of Ireland, Galway on August 20, 2025

niches in turf-dominated subregions (Fig. 2). While other studies have shown that habitats with different functional forms of macroalgae can host differing food web structures (*15*, *54*), we demonstrate that the kelp-to-turf state shift—now a global phenomenon—can strongly alter trophic interactions for generalist predators.

Without analyses of prey availability and fish diets, our study cannot resolve the specific mechanism(s) driving the larger fish niche breadth on kelp-dominated reefs or whether the rise in turf algae causes changes to fish foraging behavior (*55*) versus changes in prey availability. Nevertheless, the patterns we observed support the idea that kelp forests broadly offer a more diverse array of resources to predatory fishes compared to reefs now dominated by turf algae, even for generalists that can adapt to highly variable conditions. Thus, they suggest that subsurface canopy kelps in the North Atlantic are foundational in supporting some food web related ecosystem functions similar to trees, corals, seagrasses, and surface-reaching canopy-forming kelps (*17*, *56*–*58*).

Kelp-derived energy is important to Northwest Atlantic rocky reefs

Alongside their role as structural habitat, kelps have fast growth rates and can serve as an important basal energy source to coastal food webs when consumed by herbivores, filter feeders, and detritivores alike (*16*, *59*, *60*). The interplay between benthic (kelp-based) energy channels and pelagic (phytoplankton-based) energy channels can be important for stabilizing coastal food webs, as different channels may be productive at different times, and each has different turnover rates (*2*). However, tracing the utilization of kelp-derived energy in kelp forest food webs, particularly through multiple trophic levels, has been limited to date [but see (*37*, *60*–*62*)]. This is due, in large part, to the significant variability in bulk tissue $\delta^{13}C$ and $\delta^{15}N$ values at the base of food webs [e.g., (*11*, *47*)] as well as variability in isotopic changes with trophic transfer (*48*), leading to high uncertainty in bulk tissue isotopic estimates of kelp-derived energy acquired by consumers (*63*).

Our study shows that supplying energy to coastal food webs is an important ecosystem function of kelp forests in the Northwest Atlantic. By analyzing $\delta^{13}C$ values of EAA ($\delta^{13}C_{EAA}$; Fig. 3), we find that predatory fishes in Maine's kelp forests (indirectly) derive most of their energy from kelps (Fig. 4). Unexpectedly, we also found that fishes used 10 to 40% kelp-derived energy even when kelp biomass was low (Casco Bay and Midcoast). This pattern may reflect rapid local turnover of kelp (therefore not reflected in live standing kelp biomass) or material flux from adjacent habitats (inshore kelps and/or intertidal brown seaweeds). These stable isotope data integrate across all of the many consumer-prey interactions that occurred to transfer energy from kelp to these predatory fishes (*2*, *18*). Hence, the high proportion of predator biomass founded on kelp-based energy in our study suggests that subsurface canopy kelps are critical to the functioning of the broader food web.

The shift to turf algae rewires energy flow pathways

Critically, we observed that an abrupt loss of kelp forests due to rapid ocean warming has led to a declining availability of kelp-derived energy in the southwestern subregions of Maine. The result is a reduction in the diversity of energy channels that are powering these rocky reef food webs. We found that this change in basal resource availability reduced the amount of kelp-derived energy used by predatory fishes, and rather than shifting to use energy derived from red macroalgae, these fishes now instead rely more heavily on pelagic, phytoplankton-based energy (Fig. 4). Generalist predators' ability to occupy different habitats (i.e., kelp forests and turf reefs) and integrate a diversity of available resources makes them effective indicators of energetic rewiring of local food webs (*64*). Thus, our measured $\delta^{13}C_{EAA}$ of pollock and cunner provide a holistic picture of shifting energy pathways, integrating across all changes occurring at both the basal resource level and intermediate trophic levels.

Kelp-to-turf state shifts are a relatively new phenomenon on temperate reefs, and the consequences for food web structure remain understudied. The only other study to quantify changes in energy flow to consumers following a kelp-to-turf state shift took place in western Australia, where red turf algae became a primary energy source for herbivores, replacing kelp as a benthic energy source within the food web. However, this transition was driven by the arrival of tropical grazing fish species, which reshaped the consumer community alongside kelp loss (*25*). In contrast, we found that fish species composition in the Gulf of Maine remained unchanged with kelp decline (Fig. 1G), and this persistence of a generalist assemblage may be a common feature of the kelp-to-turf transition in higher-latitude temperate regions (*33*). Our results suggest that without an influx of new species, food web rewiring may be driven by changes in interaction strengths of existing energy channels rather than species replacement (*64*). Specifically, we observed a decline in kelp-derived energy and a concomitant increase in pelagic-derived energy on rapidly warming reefs, without major contributions from red macroalgae as an alternative benthic energy source. These findings highlight the importance of local ecological context in shaping food web responses to kelp loss, which may lead to regionally variable outcomes.

Although we found a marked difference in the structure of energy channels underlying kelp forest and turf reef food webs, we could not establish a direct relationship between energy use and fish productivity. Our methods discerned the proportion of energy that fishes acquired from various sources (Fig. 4), not the absolute quantities of energy that were conferred to secondary production on kelp-dominated versus turf-dominated reefs. Thus, the consequences of a shift from benthic to pelagic energy use on turf reefs warrant further investigation with respect to its effects on fish physiology and population biology (density, condition, per capita biomass, and turnover). Because ecological theory suggests that consumer overreliance on a single energy channel may cause food web instability, it is important to consider not only species diversity but also energy channel diversity when examining the impacts of climate change on food web resilience (*2*). It is possible that phytoplankton, a ubiquitous energy resource in coastal zones, may mitigate the loss of benthic resources (*65*). Yet, as phytoplankton productivity has been declining in the Gulf of Maine over the past 20 years (*66*), energy channel diversity may become increasingly important for maintaining nearshore food web structure (*34*).

Broader implications for climate change research and ecosystem sustainability

Last, and most broadly, we documented a previously unrecognized effect of climate change in temperate marine environments. Globally, red turf algae have proliferated over the past two decades in areas of rapid ocean warming (*23*), yet the ecological impacts of this state shift, especially with respect to animal communities and food web structure, are underexplored. Our study shows that a warming-induced

Downloaded from https://www.science.org at National University of Ireland, Galway on August 20, 2025

shift to turf algae fundamentally reshapes the availability of energy and its utilization by predators. Further, it highlights the importance of kelp—even those species that do not form large, surface-reaching canopies—in structuring fish niches (trophic dynamics) and energy use. Yet, our findings also parallel those seen in disparate ecosystems (*64*), ranging from terrestrial forests (*67*, *68*) to tropical coral reefs (*56*), indicating that climate change is exerting strong, indirect effects on food webs via habitat modification. Hence, curbing global carbon emissions and preserving foundation species will be essential for maintaining global ecosystem functioning—including diverse energy pathways—in the Anthropocene.

MATERIALS AND METHODS

Study location and experimental design

The Gulf of Maine is a semi-enclosed ocean basin in the Northwest Atlantic. Here, cool water upwells in northeast Maine and warms as it flows southwest in the Maine coastal current, creating a strong temperature differential along the coast during the summer (*69*). In response to rapid ocean warming in the region, kelp forests in southwestern Maine have collapsed and been replaced by filamentous red turf algae (*24*), whereas forests are still prevalent in the cooler, northeast subregions (*32*). Our study took place in four subregions of the Maine coast that span this gradient of temperature and habitat condition: Casco Bay (43.680, −70.050), Midcoast (43.794, −69.644), Penobscot Bay (44.099, −68.700), and Downeast (44.497, −67.620) (Fig. 1A). We defined subregions based on hydrography, geography, and local convention [see Suskiewicz *et al.* (*32*)]. At each study site ($n = 3$ to 5 per subregion), we conducted surveys to quantify available basal resources (macroalgae) and characterize the fish assemblage. We then collected representative primary producers and the two dominant fish species for stable isotope analysis. We analyzed these fishes using both bulk tissue and compound-specific stable isotope analyses to document fish isotopic niches and energy use on kelp-dominated versus red turf algae–dominated reefs.

Characterizing floral and faunal communities

Macroalgae surveys

During the summers of 2021 and 2022, we characterized macroalgae assemblages on subtidal rocky reefs via scuba ($n = 11$ to 16 sites per year and 3 to 5 sites per subregion). At each site, the divers laid a 40-m transect along the isobath at 5- to 7-m depth, parallel to shore, and then placed 1-m^2 quadrats ($n = 4$ to 6 quadrats per site) at predetermined intervals along the transect. We collected all kelps (canopy-forming brown macroalgae in the order Laminariales) from the 1-m^2 quadrat and all understory macroalgae (i.e., the diverse consortium of bladed, foliose, and filamentous seaweed taxa residing under the canopy) from a $^1/_4$ m^2 area of the quadrat. In the laboratory, we sorted macroalgae, identified them to the lowest possible taxonomic level, dried them by spinning, and weighed each group. We performed these surveys between July and mid-September (oceanographic summer) of both years.

Fish surveys

To characterize the mobile reef fish assemblage at each site, we conducted visual surveys. While swimming along 40-m transects ($n = 3$ per site), a diver identified, counted, and estimated the size (total length, 2.5-cm size bins) of each fish that they observed within a 2-m-wide band. We calculated the biomass of each fish observation via species-specific length-weight relationships from FishBase (*70*). Fish surveys were performed at the same time as macroalgae surveys in each subregion ($n = 11$ to 16 sites per year and 3 to 5 sites per subregion) between July and September of each year.

Isotope sample collection and processing

Collecting primary producer samples

On the basis of our macroalgae data and observations of the ecosystem, we determined that two potential benthic energy channels (i.e., bottom-associated, functionally distinct primary producer groups) could exist on shallow, subtidal rocky reefs in the Gulf of Maine: one based on "kelps" (canopy-forming brown macroalgae, including subtidal Laminariales and intertidal fucoids) and another based on red macroalgae (seaweeds in the phylum Rhodophyta). To characterize the isotopic values of these possible energy sources, abundant macroalgae were collected by hand via scuba, concurrent with macroalgae biomass collections. For subtidal kelps ($n = 19$; e.g., *L. digitata* and *S. latissima*), we took samples from clean parts of the interior blade, ~15 cm distal to the growth meristem. For all other macroalgae ($n = 44$), we selected whole thalli that were free of fouling. To comprehensively characterize the isotopic signature of all abundant basal energy sources, we supplemented our subtidal kelp samples with fucoidian brown macroalgae (*Ascophyllum nodosum* and *Fucus* spp.; $n = 6$) that were ubiquitous in intertidal habitats adjacent to our subtidal study sites. Because fucoids and kelps share some ecological functions and can have similar isotopic signatures, we included the fucoid samples in the "kelp" isotope end-member group. All macroalgae samples were carefully rinsed with deionized (DI) water to remove epifauna.

To characterize the isotopic signature of local phytoplankton (which constitute a pelagic energy channel), we collected particulate organic matter (POM) from 1-m depth with a Niskin sampler at sites ~1 to 5 km offshore in all subregions ($n = 27$). We prefiltered water through an inline 300-μm nitex mesh filter to remove zooplankton or large particulates. In the laboratory, we collected POM by passing 2.5 to 4.4 liters of water through precombusted glass fiber filters (GF/F, 0.7-μm mesh size) with a vacuum filter. We sequenced the DNA from a portion of several POM filters (18*S* metabarcoding) to confirm that phytoplankton comprised the bulk of the organic material trapped on the filter (see Supplementary Text and figs. S5 and S6). Hence, we refer to POM as "phytoplankton" here and elsewhere for simplicity.

Collecting consumer tissue samples

To characterize the isotopic signatures of common primary consumers, we collected samples of invertebrates that represented three distinct primary consumer guilds and may serve as fish prey. For this, we focused on filter-feeding bivalves (blue mussels *Mytilus edulis* and rock borer clams *Hiatella arctica*), grazing snails (*Lacuna vincta* and *Margarites helicinus*), and amphipods (which span a variety of families but are largely detritivores or surface suspension feeders) (*71*). These organisms ($n = 3$ to 43 samples per group per subregion) were collected in the late summer of 2022. Divers collected mussels by hand via scuba, and all small epifaunal mesoinvertebrates were collected from macroalgae by rinsing macroalgae in DI water in the laboratory and catching the contents in a 500-μm sieve. To isolate mesoinvertebrates, we looked through the contents of the sieve under a dissecting microscope and sorted mesoinvertebrates based on lowest identifiable taxonomic level (often species level for bivalves and snails, and family or superfamily for amphipods). We were careful to remove pieces of detritus or macroalgae from mesoinvertebrates.

Downloaded from https://www.science.org at National University of Ireland, Galway on August 20, 2025

Invertebrates were frozen after collection. Tissue samples from *Mytilus* were obtained by dissecting a piece of the adductor muscle. We processed whole snails and *Hiatella* as bulk samples and subjected them to a demineralization in weak (0.5 M) hydrochloric acid for 12 to 24 hours to remove calcium from their shells. We then extracted lipids from all invertebrate samples by soaking them for 24 hours in a 2:1 chloroform:methanol solution. After three rounds of soaking (72 hours total), exchanging the chloroform:methanol solution between rounds, we thoroughly rinsed samples in DI water.

We collected fishes from rocky reefs in Casco Bay, Midcoast, Penobscot Bay, and Downeast subregions between September and November of 2022. We used hook and line fishing to target pollock ($n = 10$ to 14 per subregion) and deployed minnow traps baited with mussels to catch cunner ($n = 5$ to 15 per subregion). Fishes were euthanized in the field using an MS-222 seawater solution in accordance with the University of Maine Institutional Animal Care and Use Committee (IACUC) (protocol A2022-08-02). Specimens were temporarily stored on ice and then dissected in the laboratory the same day they were caught. We excised a piece of dorsal muscle tissue for isotopic analysis, which was rinsed with DI water and stored frozen. As with invertebrate tissues, we lipid extracted fish tissues with a 2:1 chloroform:methanol solution for 72 hours and then rinsed them with DI water.

We stored samples in muffled 20-ml scintillation vials (borosilicate glass with foil-lined caps). All samples were kept frozen at −20°C until they were lyophilized.

Bulk tissue $\delta^{13}C$ and $\delta^{15}N$ analysis

We packed dried tissue samples into 3.5 mm–by–5 mm tin capsules (Analytics, Valencia, CA; USA Analytics, Anaheim, CA) to prepare them for bulk tissue $\delta^{13}C$ and $\delta^{15}N$ analysis. We weighed kelp and other macroalgae samples to ~3.5 mg and invertebrate samples and fish muscle to ~1 mg. For phytoplankton samples, we packed ~$^1/_4$ to $^1/_2$ of each GF/F filter into 5 mm–by–9 mm tin capsules.

Bulk tissue $\delta^{13}C$ and $\delta^{15}N$ values were measured via continuous flow on a Costech 4010 elemental analyzer coupled to a Thermo Fisher Scientific DELTA V Plus isotope ratio mass spectrometer (EA-IRMS) at the University of New Mexico Center for Stable Isotopes (UNM-CSI; Albuquerque, New Mexico, USA). We report all isotope results as δ values with units of per mil (‰)

$$\delta^{13}C \text{ or } \delta^{15}N = \left[\left(R_{sample}/R_{standard}\right) - 1\right] \times 1000$$

where R represents the ^{13}C:^{12}C or ^{15}N:^{14}N ratios (*72*). The internationally accepted standards are Vienna Pee Dee Belemnite for $\delta^{13}C$ and atmospheric N_2 for $\delta^{15}N$. The isotopic values of our samples were corrected and calibrated to these international standards based on the analysis of in-house reference materials (casein and tuna for protein and green chile and blue gramma for plants/algae) that had SDs below 0.2‰ within all runs.

Stable carbon isotope analysis of EAAs ($\delta^{13}C_{EAA}$)

We used $\delta^{13}C_{EAA}$ fingerprinting to assess the energy (carbon) contribution of basal resources to fish from the four subregions across the coast of Maine. To prepare samples for $\delta^{13}C_{EAA}$ analysis, we subjected them to hydrolysis, derivatization, and analysis in a gas chromatography combustion unit coupled to an IRMS (GC-C-IRMS). First, we hydrolyzed macroalgae samples (4 to 5 mg), POM filters (~$^1/_4$ to $^1/_2$ filter), and lipid-extracted fish muscle (5 to 6 mg) in 6 M hydrochloric acid. We flushed hydrolysis tubes with N_2 gas before sealing and incubated them for 20 hours at 110°C. Hydrolyzed amino acids from primary producer samples were subsequently filtered through muffled quartz wool to remove any remaining particulates.

We derivatized amino acids into *N*-trifluoroacetyl isopropyl esters following Silfer *et al.* (*73*). Hydrolysates were subsequently dried under N_2, esterified in 1 ml of 4:1 isopropanol:acetyl chloride (105°C, 1 hour), dried again under N_2 with two rinse cycles using dichloromethane (DCM), and then acetylated in 1 ml of 1:1 trifluoroacetic anhydride:DCM (105°C, 10 min). All samples for this project were derivatized in batches of 8 to 25 samples, along with an in-house reference material containing amino acids with known $\delta^{13}C$ values measured via EA-IRMS at UNM-CSI (table S5).

The in-house reference material was a mixture of 12 purified and powdered amino acids (Sigma-Aldrich, Saint Louis, MO, USA): alanine, aspartic acid, glutamic acid, glycine, isoleucine, leucine, lysine, phenylalanine, proline, serine, threonine, and valine. To make the reference material, we dissolved amino acid powders into weak hydrochloric acid (< 0.01 M) at a concentration of ~125 mM. Individual amino acid solutions were then mixed together, and a small aliquot of this mixture was dried under N_2 gas and derivatized alongside each batch of unknown samples.

We analyzed our derivatized samples and in-house reference material via a GC-C-IRMS at UNM-CSI. Briefly, we injected 1 to 1.5 µl of each sample into a 60-m BPX5 gas chromatograph column (0.32-mm internal diameter and 1-µm film thickness; SGE Analytical Science) within a Trace 1310 GC, where amino acid separation was completed, then combusted into CO_2 within a high temperature furnace (1000°C) of Thermo Fisher Scientific IsoLink II, and finally analyzed in a Thermo Fisher Scientific DELTA V Plus IRMS. We ran all samples in duplicate or triplicate injections, taking the average isotopic values of each sample. The within-run SDs of all amino acid $\delta^{13}C$ values for the in-house reference material measured in this study ranged from 0.2‰ (alanine) to 0.5‰ (lysine) but averaged < 0.5‰ per day, as averaged across three to seven injections. The global SDs ranged from 0.5‰ (valine) to 1.3‰ (phenylalanine) across all runs and standard injections (table S5).

$\delta^{13}C$ values were then corrected on the basis of measurements of the in-house reference material (table S5), which was analyzed bracketing each sample and at the beginning and end of each run. The reagents used during derivatization add carbon to the side chains of amino acids, and $\delta^{13}C$ values measured via GC-C-IRMS are thus a combination of intrinsic amino acid carbon and reagent carbon. However, because amino acid reference materials of known $\delta^{13}C$ composition were derivatized and run with each batch of samples, we were able to correct for this carbon addition for each amino acid using the following equation

$$\delta^{13}C_{sample} = \frac{\left(\delta^{13}C_{dsa} - \delta^{13}C_{dst} + \delta^{13}C_{std} \times p_{std}\right)}{p_{std}}$$

Here, $\delta^{13}C_{dsa}$ refers to the measured value of a derivatized amino acid within the sample, and $\delta^{13}C_{dst}$ is the measured value of the derivatized amino acid within the in-house reference material. The term $\delta^{13}C_{std}$ reflects the underivatized or intrinsic $\delta^{13}C$ value of that amino acid in the reference material; these values were determined via EA-IRMS at UNM-CSI (table S5). Last, p_{std} is the proportion of carbon in the measured derivative that was originally sourced from the amino acid, which varies among amino acids. These corrections

Downloaded from https://www.science.org at National University of Ireland, Galway on August 20, 2025

were done on a daily or on a "per run" basis, which means that unknown samples were corrected using four to six bracketed injections of the reference material.

We generated $\delta^{13}C$ values for 12 amino acids; however, our analyses focused on five of six EAAs that we could reliably measure in our primary producers: threonine, valine, leucine, isoleucine, and phenylalanine. These compounds are useful for tracing the movement of organic matter across food webs, as they are not synthesized or modified by consumers and thus do not undergo discrimination as they move between trophic levels (*51*, *52*). We did not use data for amino acids in samples where SDs exceeded 1.0‰ among injections. In addition, although lysine is considered essential and was measured, this EAA exhibited significant coelution with tyrosine in many of our primary producer samples, resulting in variable $\delta^{13}C$ values. Hence, we did not include lysine data in any statistical analyses.

Statistical analyses

All statistical analyses were done in R (version 4.2.2) (*74*).

Variation in basal resource availability

We grouped macroalgae biomass data based on broad taxonomic and morphological categories (Fig. 1, E and F) and summarized group biomass by site and survey date. We used a JT trend test—an extension of a nonparametric rank test that evaluates whether samples from ordered groups come from different distributions—to test two hypotheses about trends in macroalgae biomass by subregion (R package "clinfun") (*75*, *76*) based on a priori knowledge (*32*). We ran these and all subsequent JT trend tests with 999 permutations. First, we tested whether the relative biomass of kelp significantly decreased as reefs transitioned from kelp-to-turf dominance. Next, we tested whether the relative biomass of red macroalgae (which includes all rhodophytes) and turf algae [defined as those red macroalgae species with filamentous or uniseriate morphologies (*77*)] increased along the same gradient of habitat condition (table S1). For these tests, we coded "subregion" as an ordered categorical predictor with Downeast as our kelp forest subregion, ranked as "1," followed by Penobscot Bay ("2"), Midcoast ("3"), and Casco Bay ("4").

Variation in fish biomass

We summed the total estimated fish biomass observed on each transect and tested whether biomass varied in accordance with the subregional kelp-to-turf gradient with a JT trend test. As above, we ordered subregions 1 to 4 from Downeast to Casco Bay. We ran this trend test with no directional hypothesis to test for either increasing or decreasing fish biomass along the coast (table S1).

Variation in macroalgae bulk tissue $\delta^{13}C$ and $\delta^{15}N$

To determine whether the isotopic values of basal resources vary by broad primary producer group (kelp, red macroalgae, and POM), we performed KW tests for $\delta^{13}C$ and $\delta^{15}N$ values separately, with post hoc Dunn tests [R package "dunn.test" (*78*)] of which groups had different isotopic values (Supplementary Text and table S2). To evaluate whether there are systematic trends in $\delta^{13}C$ and $\delta^{15}N$ values across subregions, we ran JT trend tests as above without a directional hypothesis for each group of macroalgae, invertebrate, and fish (Supplementary Text and table S2).

Fish isotopic niche width and overlap

For predatory fishes, the focal group of this study, we used SIBER [R package "siber" (*46*)] to assess the isotopic niche area of the whole assemblage and compare each species' niche breadth between subregions. We calculated the SEA-B for isotopic niches with the default parameters of 20,000 model iterations, discarding the first 1000 values, running two chains, and setting vague normal priors. Reported SEA-B is based on predicted ellipses that contain 40% of data. We also compared isotopic niche overlap by running pairwise KW tests on cunner and pollock for $\delta^{13}C$ and $\delta^{15}N$ values (Fig. 2, Supplementary Text, fig. S3, and table S3) and noted where there is isotopic niche overlap or separation.

Partitioning primary producer groups with a classification model

To determine whether $\delta^{13}C_{EAA}$ could distinguish kelp ($n = 16$), red macroalgae ($n = 17$), and phytoplankton ($n = 11$)—the three primary producer groups that represent distinct energy channels in our system—we used a FDA, a nonparametric classification model. We applied the FDA [R package "mda" (*79*)] using $\delta^{13}C_{EAA}$ from five EAAs (isoleucine, leucine, phenylalanine, threonine, and valine) as predictors and assessed the robustness of producer fingerprints based on successful reclassification in a leave-one-out cross-validation test. Kelps, red macroalgae, and phytoplankton were sufficiently separated in multivariate $\delta^{13}C_{EAA}$ space (see Results, Fig. 3, and table S6), and thus, we used this FDA model for quantifying energy contributions to consumers.

For comparative purposes, we also applied a linear discriminant analysis (LDA), which is a robust model often used for classifying producer groups from $\delta^{13}C_{EAA}$ data (*18*, *50*, *80*). We ran an LDA on primary producer $\delta^{13}C_{EAA}$ data [R package "MASS" (*81*)] and, as above, assessed the fidelity with a leave-one-out cross-validation test. LDA correctly classified producer samples as kelps, phytoplankton, or red macroalgae with 89% success (fig. S7 and table S7). However, LDA has assumptions of multivariate normality and homogeneity of group variances. The $\delta^{13}C$ values of one EAA (leucine) were not normally distributed; therefore, our dataset did not meet the model assumptions. We report the LDA results for consistency with previous studies and for comparison to the FDA (fig. S7); however, we used only the FDA for our core analysis and interpretation of consumer energy acquisition (Fig. 4).

Quantifying consumers' basal energy sources

To quantify the proportion of energy from each producer group acquired by fishes, we used a bootstrap resampling approach to run 10,000 iterations of the FDA model with a random subset of 10 members of each producer group each time (sampled with replacement). We used each iteration of the model to classify fishes based on their $\delta^{13}C_{EAA}$, with the model returning a probability that each individual fish belonged to each producer group. We averaged these posterior probability estimates from all 10,000 iterations to get a mean estimate for each individual (table S4) and used those mean probabilities of classification as the estimated proportion of energy derived from each producer group (*18*). We chose to use this multivariate statistical method (FDA) rather than the traditional Bayesian mixing models [e.g., "MixSIAR" (*82*)] because they can more effectively use multiple EAA to partition the proportional contribution of multiple basal resource groups (*18*). $\delta^{13}C_{EAA}$ data naturally avoid the common issues associated with bulk tissue isotopic data (where mixing models are common and useful). Notably, multivariate isotopic patterns of marine algae are conserved across broad spatiotemporal scales (*52*), and EAAs have negligible isotopic offsets with trophic transfer in most cases (*51*, *83*).

We summarized the proportion of energy that fishes derived from each of the three producer groups. As above, we used JT trend tests to analyze whether trends in consumer use of kelp-, red macroalgae-,

Downloaded from https://www.science.org at National University of Ireland, Galway on August 20, 2025

and phytoplankton-derived energy increased or decreased across the four subregions.

Supplementary Materials

This PDF file includes:

Supplementary Text
Figs. S1 to S7
Tables S1 to S7
Legends for data files S1 to S6
References

REFERENCES AND NOTES

1. R. L. Lindeman, The trophic-dynamic aspect of ecology. *Ecology* **23**, 399–417 (1942).
2. N. Rooney, K. McCann, G. Gellner, J. C. Moore, Structural asymmetry and the stability of diverse food webs. *Nature* **442**, 265–269 (2006).
3. Z. Zhou, V. Krashevska, R. Widyastuti, S. Scheu, A. Potapov, Tropical land use alters functional diversity of soil food webs and leads to monopolization of the detrital energy channel. *eLife* **11**, e75428 (2022).
4. J. P. Benstead, C. M. Pringle, Deforestation alters the resource base and biomass of endemic stream insects in eastern Madagascar. *Freshw. Biol.* **49**, 490–501 (2004).
5. A. B. Navarro, M. Magioli, J. A. Bogoni, L. F. Silveira, M. Z. Moreira, E. R. Alexandrino, D. T. A. Da Luz, W. R. Silva, M. A. Pizo, V. C. De Oliveira, K. M. P. M. D. B. Ferraz, Isotopic niches of tropical birds reduced by anthropogenic impacts: A 100-year perspective. *Oikos* **130**, 1892–1904 (2021).
6. R. Karkarey, T. Alcoverro, S. Kumar, R. Arthur, Coping with catastrophe: Foraging plasticity enables a benthic predator to survive in rapidly degrading coral reefs. *Anim. Behav.* **131**, 13–22 (2017).
7. T. N. Hempson, N. A. J. Graham, M. A. MacNeil, D. H. Williamson, G. P. Jones, G. R. Almany, Coral reef mesopredators switch prey, shortening food chains, in response to habitat degradation. *Ecol. Evol.* **7**, 2626–2635 (2017).
8. R. S. Steneck, M. H. Graham, B. J. Bourque, D. Corbett, J. M. Erlandson, J. A. Estes, M. J. Tegner, Kelp forest ecosystems: Biodiversity, stability, resilience and future. *Environ. Conserv.* **29**, 436–459 (2002).
9. H. Christie, K. Norderhaug, S. Fredriksen, Macrophytes as habitat for fauna. *Mar. Ecol. Prog. Ser.* **396**, 221–233 (2009).
10. H. Teagle, S. J. Hawkins, P. J. Moore, D. A. Smale, The role of kelp species as biogenic habitat formers in coastal marine ecosystems. *J. Exp. Mar. Biol. Ecol.* **492**, 81–98 (2017).
11. E. A. Elliott Smith, M. D. Fox, Characterizing energy flow in kelp forest food webs: A geochemical review and call for additional research. *Ecography* **2022**, e05566 (2022).
12. P. K. Dayton, "Toward an understanding of community resilience and the potential effects of enrichments to the benthos at McMurdo Sound, Antarctica," in *Proceedings of the Colloquium on Conservation Problems in Antarctica* (1972), Allen Press, pp. 81–96.
13. A. W. Ebeling, R. J. Larson, W. S. Alevizon, R. N. Bray, Annual variability of reef-fish assemblages in kelp forests off Santa Barbara, California. *Fish. Bull.* **78**, 361–377 (1980).
14. A. C. Davenport, T. W. Anderson, Positive indirect effects of reef fishes on kelp performance: The importance of mesograzers. *Ecology* **88**, 1548–1561 (2007).
15. A. Angel, F. Ojeda, Structure and trophic organization of subtidal fish assemblages on the northern Chilean coast: The effect of habitat complexity. *Mar. Ecol. Prog. Ser.* **217**, 81–91 (2001).
16. D. O. Duggins, C. A. Simenstad, J. A. Estes, Magnification of secondary production by kelp detritus in coastal marine ecosystems. *Science* **245**, 170–173 (1989).
17. M. H. Graham, Effects of local deforestation on the diversity and structure of Southern California giant kelp forest food webs. *Ecosystems* **7**, 341–357 (2004).
18. E. A. Elliott Smith, C. Harrod, F. Docmac, S. D. Newsome, Intraspecific variation and energy channel coupling within a Chilean kelp forest. *Ecology* **102**, e03198 (2021).
19. K. Filbee-Dexter, R. Scheibling, Sea urchin barrens as alternative stable states of collapsed kelp ecosystems. *Mar. Ecol. Prog. Ser.* **495**, 1–25 (2014).
20. J. G. Smith, D. Malone, M. H. Carr, Consequences of kelp forest ecosystem shifts and predictors of persistence through multiple stressors. *Proc. R. Soc. B* **291**, 20232749 (2024).
21. R. W. Markel, J. B. Shurin, Indirect effects of sea otters on rockfish (*Sebastes* spp.) in giant kelp forests. *Ecology* **96**, 2877–2890 (2015).
22. S. S. Gabara, B. H. Konar, M. S. Edwards, Biodiversity loss leads to reductions in community-wide trophic complexity. *Ecosphere* **12**, e03361 (2021).
23. K. Filbee-Dexter, T. Wernberg, Rise of turfs: A new battlefront for globally declining kelp forests. *Bioscience* **68**, 64–76 (2018).
24. J. A. Dijkstra, L. G. Harris, K. Mello, A. Litterer, C. Wells, C. Ware, Invasive seaweeds transform habitat structure and increase biodiversity of associated species. *J. Ecol.* **105**, 1668–1678 (2017).
25. A. Pessarrodona, K. Filbee-Dexter, T. Alcoverro, J. Boada, C. J. Feehan, S. Fredriksen, S. P. Grace, Y. Nakamura, C. A. Narvaez, K. M. Norderhaug, T. Wernberg, Homogenization and miniaturization of habitat structure in temperate marine forests. *Glob. Chang. Biol.* **27**, 5262–5275 (2021).
26. A. Pessarrodona, J. Assis, K. Filbee-Dexter, M. T. Burrows, J.-P. Gattuso, C. M. Duarte, D. Krause-Jensen, P. J. Moore, D. A. Smale, T. Wernberg, Global seaweed productivity. *Sci. Adv.* **8**, eabn2465 (2022).
27. T. Wernberg, D. A. Smale, F. Tuya, M. S. Thomsen, T. J. Langlois, T. de Bettignies, S. Bennett, C. S. Rousseaux, An extreme climatic event alters marine ecosystem structure in a global biodiversity hotspot. *Nat. Clim. Change* **3**, 78–82 (2013).
28. A. Pessarrodona, A. Vergés, N. E. Bosch, S. Bell, S. Smith, M. P. Sgarlatta, T. Wernberg, Tropicalization unlocks novel trophic pathways and enhances secondary productivity in temperate reefs. *Funct. Ecol.* **36**, 659–673 (2022).
29. S. Connell, B. Russell, D. Turner, S. Shepherd, T. Kildea, D. Miller, L. Airoldi, A. Cheshire, Recovering a lost baseline: Missing kelp forests from a metropolitan coast. *Mar. Ecol. Prog. Ser.* **360**, 63–72 (2008).
30. L. Airoldi, E. Ballesteros, R. Buonuomo, J. van Belzen, T. J. Bouma, E. Cebrian, O. de Clerk, A. H. Engelen, F. Ferrario, S. Fraschetti, F. Gianni, P. Guidetti, L. Ivesa, F. P. Mancuso, F. Micheli, S. Perkol-Finkel, E. A. Serrao, E. M. Strain, L. Mangialajo, "Marine forests at risk: Solutions to halt the loss and promote the recovery of Mediterranean canopy-forming seaweeds," in *Proceedings of the 5th Mediterranean Symposium on Marine Vegetation* (2014), pp. 28–33.
31. F. E. Moy, H. Christie, Large-scale shift from sugar kelp (*Saccharina latissima*) to ephemeral algae along the south and west coast of Norway. *Mar. Biol. Res.* **8**, 309–321 (2012).
32. T. S. Suskiewicz, J. E. K. Byrnes, R. S. Steneck, R. Russell, C. J. Wilson, D. B. Rasher, Ocean warming undermines the recovery resilience of New England kelp forests following a fishery-induced trophic cascade. *Ecology* **105**, e4334 (2024).
33. H. Christie, G. S. Andersen, L. A. Tveiten, F. E. Moy, Macrophytes as habitat for fish. *ICES J. Mar. Sci.* **79**, 435–444 (2022).
34. N. Rooney, K. S. McCann, Integrating food web diversity, structure and stability. *Trends Ecol. Evol.* **27**, 40–46 (2012).
35. R. S. Steneck, J. Vavrinec, A. V. Leland, Accelerating trophic-level dysfunction in kelp forest ecosystems of the western North Atlantic. *Ecosystems* **7**, 323–332 (2004).
36. J. D. Witman, K. P. Sebens, Regional variation in fish predation intensity: A historical perspective in the Gulf of Maine. *Oecologia* **90**, 305–315 (1992).
37. J. Udy, S. Wing, S. O'Connell-Milne, L. Durante, R. McMullin, S. Kolodzey, R. Frew, Regional differences in supply of organic matter from kelp forests drive trophodynamics of temperate reef fish. *Mar. Ecol. Prog. Ser.* **621**, 19–32 (2019).
38. R. Rangeley, D. Kramer, Use of rocky intertidal habitats by juvenile pollock *Pollachius virens*. *Mar. Ecol. Prog. Ser.* **126**, 9–17 (1995).
39. F. Patricio Ojeda, J. H. Dearborn, Feeding ecology of benthic mobile predators: Experimental analyses of their influence in rocky subtidal communities of the Gulf of Maine. *J. Exp. Mar. Biol. Ecol.* **149**, 13–44 (1991).
40. Bigelow and Schroeder's Fishes of the Gulf of Maine, Third Edition, B. B. Collette, G. Klein-Macphee, Eds. (Smithsonian Books, 2002); https://kewandwillow.com/book/9781560989516.
41. B. L. Olla, A. J. Bejda, A. D. Martin, Activity, movements, and feeding behavior of the cunner, *Tautogolabrus adspersus*, and comparison of food habits with young tautog, *Tautoga onitis*, off Long Island, New York. *Fish. Bull.* **73**, (1975).
42. J. M. Green, G. Martel, D. W. Martin, Comparisons of the feeding activity and diets of male and female cunners *Tautogolabrus adspersus* (Pisces: Labridae). *Mar. Biol.* **84**, 7–11 (1984).
43. J. A. Raven, A. M. Johnston, J. E. Kübler, R. Korb, S. G. McInroy, L. L. Handley, C. M. Scrimgeour, D. I. Walker, J. Beardall, M. Vanderklift, S. Fredriksen, K. H. Dunton, Mechanistic interpretation of carbon isotope discrimination by marine macroalgae and seagrasses. *Funct.Plant Biol.* **29**, 355–378 (2002).
44. M. F. Leggett, O. Johannsson, R. Hesslein, D. G. Dixon, W. D. Taylor, M. R. Servos, Influence of inorganic nitrogen cycling on the δ^{15}N of Lake Ontario biota. *Can. J. Fish. Aquat. Sci.* **57**, 1489–1496 (2000).
45. S. D. Newsome, C. Martinez del Rio, S. Bearhop, D. L. Phillips, A niche for isotopic ecology. *Front. Ecol. Environ.* **5**, 429–436 (2007).
46. A. L. Jackson, R. Inger, A. C. Parnell, S. Bearhop, Comparing isotopic niche widths among and within communities: SIBER—Stable Isotope Bayesian Ellipses in R. *J. Anim. Ecol.* **80**, 595–602 (2011).
47. M. Dethier, E. Sosik, A. Galloway, D. Duggins, C. Simenstad, Addressing assumptions: Variation in stable isotopes and fatty acids of marine macrophytes can confound conclusions of food web studies. *Mar. Ecol. Prog. Ser.* **478**, 1–14 (2013).
48. R. B. Stephens, O. N. Shipley, R. J. Moll, Meta-analysis and critical review of trophic discrimination factors (Δ^{13}C and Δ^{15}N): Importance of tissue, trophic level and diet source. *Funct. Ecol.* **37**, 2535–2548 (2023).
49. S. D. Newsome, M. L. Fogel, L. Kelly, C. M. Del Rio, Contributions of direct incorporation from diet and microbial amino acids to protein synthesis in Nile tilapia: Contributions of diet and microbial amino acids to protein synthesis. *Funct. Ecol.* **25**, 1051–1062 (2011).

Downloaded from https://www.science.org at National University of Ireland, Galway on August 20, 2025

50. T. Larsen, M. Ventura, N. Andersen, D. M. O'Brien, U. Piatkowski, M. D. McCarthy, Tracing carbon sources through aquatic and terrestrial food webs using amino acid stable isotope fingerprinting. *PLOS ONE* **8**, e73441 (2013).
51. K. W. McMahon, M. L. Fogel, T. S. Elsdon, S. R. Thorrold, Carbon isotope fractionation of amino acids in fish muscle reflects biosynthesis and isotopic routing from dietary protein: Carbon isotope fractionation of fish muscle amino acids. *J. Anim. Ecol.* **79**, 1132–1141 (2010).
52. E. A. E. Smith, M. D. Fox, M. L. Fogel, S. D. Newsome, Amino acid δ^{13}C fingerprints of nearshore marine autotrophs are consistent across broad spatiotemporal scales: An intercontinental isotopic dataset and likely biochemical drivers. *Funct. Ecol.* **36**, 1191–1203 (2022).
53. T. Larsen, D. L. Taylor, M. B. Leigh, D. M. O'Brien, Stable isotope fingerprinting: A novel method for identifying plant, fungal, or bacterial origins of amino acids. *Ecology* **90**, 3526–3535 (2009).
54. C. Hipólito, R. M. A. Neto, T. M. M. Costa, M. A. Dionísio, A. C. L. Prestes, J. M. N. Azevedo, G. M. Martins, A. I. Neto, Frondose and turf-dominated marine habitats support distinct trophic pathways: Evidence from ^{15}N and ^{13}C stable isotope analyses. *Arquipelago Life Mar. Sci.* **37**, 37–44 (2020).
55. B. S. O'Brien, K. Mello, A. Litterer, J. A. Dijkstra, Seaweed structure shapes trophic interactions: A case study using a mid-trophic level fish species. *J. Exp. Mar. Biol. Ecol.* **506**, 1–8 (2018).
56. P. S. Morillo-Velarde, P. Briones-Fourzán, L. Álvarez-Filip, S. Aguíñiga-García, A. Sánchez-González, E. Lozano-Álvarez, Habitat degradation alters trophic pathways but not food chain length on shallow Caribbean coral reefs. *Sci. Rep.* **8**, 4109 (2018).
57. R. H. MacArthur, J. W. MacArthur, On bird species diversity. *Ecology* **42**, 594–598 (1961).
58. Y. S. Zhang, B. R. Silliman, A facilitation cascade enhances local biodiversity in seagrass beds. *Diversity* **11**, 30 (2019).
59. K. H. Mann, Seaweeds: Their productivity and strategy for growth. *Science* **182**, 975–981 (1973).
60. S. Fredriksen, Food web studies in a Norwegian kelp forest based on stable isotope (δ^{13}C and δ^{15}N) analysis. *Mar. Ecol. Prog. Ser.* **260**, 71–81 (2003).
61. V. R. von Biela, S. D. Newsome, J. L. Bodkin, G. H. Kruse, C. E. Zimmerman, Widespread kelp-derived carbon in pelagic and benthic nearshore fishes suggested by stable isotope analysis. *Estuar. Coast. Shelf Sci.* **181**, 364–374 (2016).
62. E. A. Elliott Smith, C. Harrod, S. D. Newsome, The importance of kelp to an intertidal ecosystem varies by trophic level: Insights from amino acid δ^{13}C analysis. *Ecosphere* **9**, e02516 (2018).
63. R. J. Miller, H. M. Page, Kelp as a trophic resource for marine suspension feeders: A review of isotope-based evidence. *Mar. Biol.* **159**, 1391–1402 (2012).
64. T. J. Bartley, K. S. McCann, C. Bieg, K. Cazelles, M. Granados, M. M. Guzzo, A. S. MacDougall, T. D. Tunney, B. C. McMeans, Food web rewiring in a changing world. *Nat. Ecol. Evol.* **3**, 345–354 (2019).
65. A. C. Thomas, D. W. Townsend, R. Weatherbee, Satellite-measured phytoplankton variability in the Gulf of Maine. *Cont. Shelf Res.* **23**, 971–989 (2003).
66. W. M. Balch, D. T. Drapeau, B. C. Bowler, N. R. Record, N. R. Bates, S. Pinkham, R. Garley, C. Mitchell, Changing hydrographic, biogeochemical, and acidification properties in the Gulf of Maine as measured by the Gulf of Maine North Atlantic time series, GNATS, between 1998 and 2018. *JGR Biogeosci.* **127**, e2022JG006790 (2022).
67. A. M. Ellison, M. S. Bank, B. D. Clinton, E. A. Colburn, K. Elliott, C. R. Ford, D. R. Foster, B. D. Kloeppel, J. D. Knoepp, G. M. Lovett, J. Mohan, D. A. Orwig, N. L. Rodenhouse, W. V. Sobczak, K. A. Stinson, J. K. Stone, C. M. Swan, J. Thompson, B. Von Holle, J. R. Webster, Loss of foundation species: Consequences for the structure and dynamics of forested ecosystems. *Front. Ecol. Environ.* **3**, 479–486 (2005).
68. A. M. Potapov, N. Dupérré, M. Jochum, K. Dreczko, B. Klarner, A. D. Barnes, V. Krashevska, K. Rembold, H. Kreft, U. Brose, R. Widyastuti, D. Harms, S. Scheu, Functional losses in ground spider communities due to habitat structure degradation under tropical land-use change. *Ecology* **101**, e02957 (2020).
69. D. A. Brooks, D. W. Townsend, Variability of the coastal current and nutrient pathways in the eastern Gulf of Maine. *J. Mar. Res.* **47**, 303–321 (1989).
70. R. Froese, D. Pauly, Eds., *FishBase 2000: Concepts, Designs and Data Sources* (International Center for Living Aquatic Resources Management, 2000).
71. L. W. Pollock, *A Practical Guide to the Marine Animals of Northeastern North America* (Rutgers Univ. Press, 1998).
72. Z. Sharp, *Principles of Stable Isotope Geochemistry* (University of New Mexico, ed. 2, 2017).
73. J. A. Silfer, M. H. Engel, S. A. Macko, E. J. Jumeau, Stable carbon isotope analysis of amino acid enantiomers by conventional isotope ratio mass spectrometry and combined gas chromatography/isotope ratio mass spectrometry. *Anal. Chem.* **63**, 370–374 (1991).
74. R Core Team, *R: A Language and Environment for Statistical Computing* (R Foundation for Statistical Computing, 2022). www.R-project.org/.
75. A. R. Jonckheere, A distribution-free *k*-sample test against ordered alternatives. *Biometrika* **41**, 133–145 (1954).
76. V. E. Seshan, K. Whiting, clinfun: Clinical trial design and data analysis functions (2007). https://doi.org/10.32614/CRAN.package.clinfun.
77. S. Connell, M. Foster, L. Airoldi, What are algal turfs? Towards a better description of turfs. *Mar. Ecol. Prog. Ser.* **495**, 299–307 (2014).
78. A. Dinno, dunn.test: Dunn's test of multiple comparisons using rank sums (2014). https://doi.org/10.32614/CRAN.package.dunn.test.
79. T. Hastie, R. Tibshirani, mda: Mixture and flexible discriminant analysis (1998). https://doi.org/10.32614/CRAN.package.mda.
80. A. C. Besser, E. A. Elliott Smith, S. D. Newsome, Assessing the potential of amino acid δ^{13}C and δ^{15}N analysis in terrestrial and freshwater ecosystems. *J. Ecol.* **110**, 935–950 (2022).
81. B. Ripley, B. Venables, MASS: Support functions and datasets for Venables and Ripley's MASS (2009). https://doi.org/10.32614/CRAN.package.MASS.
82. B. Stock, B. Semmens, MixSIAR: Bayesian mixing models in R (2016). https://doi.org/10.32614/CRAN.package.MixSIAR.
83. K. W. McMahon, M. J. Polito, S. Abel, M. D. McCarthy, S. R. Thorrold, Carbon and nitrogen isotope fractionation of amino acids in an avian marine predator, the gentoo penguin (*Pygoscelis papua*). *Ecol. Evol.* **5**, 1278–1290 (2015).
84. A. M. Comeau, W. K. W. Li, J.-É. Tremblay, E. C. Carmack, C. Lovejoy, Arctic ocean microbial community structure before and after the 2007 record sea ice minimum. *PLOS ONE* **6**, e27492 (2011).
85. B. J. Callahan, P. J. McMurdie, M. J. Rosen, A. W. Han, A. J. A. Johnson, S. P. Holmes, DADA2: High-resolution sample inference from Illumina amplicon data. *Nat. Methods* **13**, 581–583 (2016).
86. B. J. Callahan, P. J. McMurdie, S. P. Holmes, Exact sequence variants should replace operational taxonomic units in marker-gene data analysis. *ISME J.* **11**, 2639–2643 (2017).
87. L. Guillou, D. Bachar, S. Audic, D. Bass, C. Berney, L. Bittner, C. Boutte, G. Burgaud, C. De Vargas, J. Decelle, J. Del Campo, J. R. Dolan, M. Dunthorn, B. Edvardsen, M. Holzmann, W. H. C. F. Kooistra, E. Lara, N. Le Bescot, R. Logares, F. Mahé, R. Massana, M. Montresor, R. Morard, F. Not, J. Pawlowski, I. Probert, A.-L. Sauvadet, R. Siano, T. Stoeck, D. Vaulot, P. Zimmermann, R. Christen, The protist ribosomal reference database (PR2): A catalog of unicellular eukaryote small sub-unit rRNA sequences with curated taxonomy. *Nucleic Acids Res.* **41**, D597–D604 (2012).

Acknowledgments: We are grateful to K. Cammen for facilitating fish sample collection permitting and to S. Newsome, L. Burkemper, and V. Atudorei for providing expertise and facilitating the isotope analyses. We thank S. Ryan, P. Churney, R. Francolini, J. Wheeler, A. Ouimet, C. Brown, P. Jekielek, S. Mann, S. Greenlee, A. Ascher, and K. Kleman for help with field surveys and/or sample collection. We thank the Downeast Institute and the Hurricane Island Center for Science and Leadership for logistical support. Last, we thank K. Cammen, K. Van Volkom, and four reviewers for thoughtful feedback that improved this manuscript. This work was conducted with permission from the Maine Department of Marine Resources (special licenses #2021-22-04 and #2022-36-03), and fish collections were made with University of Maine IACUC approval (protocol #A2022-08-02). **Funding:** This work was supported by an NSF EPSCoR award (#OIA-1849227) (D.B.R.), a Maine Sea Grant program development award (D.S.Y.), the Louise H. and David S. Ingalls Foundation (D.B.R.), and the Bigelow Laboratory for Ocean Sciences (D.B.R.). **Author contributions:** Conceptualization: D.S.Y. and D.B.R. Methodology: D.S.Y., E.A.E.S., and D.B.R. Investigation: D.S.Y., E.A.E.S., S.P.F., and D.B.R. Resources: D.S.Y., E.A.E.S., S.P.F., and D.B.R. Data curation: D.S.Y., E.A.E.S., S.P.F., and D.B.R. Data analysis: D.S.Y. and E.A.E.S. Visualization: D.S.Y. Supervision: D.B.R. Funding acquisition: D.S.Y. and D.B.R. Writing—original draft: D.S.Y., E.A.E.S., and D.B.R. Writing—review and editing: D.S.Y., E.A.E.S., S.P.F., and D.B.R. **Competing interests:** The authors declare that they have no competing interests. **Data and materials availability:** All data needed to evaluate the conclusions in the paper are present in the paper and/or the Supplementary Materials. The original data files are archived in Dryad (https://doi.org/10.5061/dryad.bcc2fqzqz). Codes used to generate the analyses and figures in this paper are available in Zenodo (https://doi.org/10.5281/zenodo.15232648) and GitHub (https://github.com/dyiu/kelp-forest-turf-reef-energy-flow).

Submitted 14 February 2025
Accepted 2 May 2025
Published 6 June 2025
10.1126/sciadv.adw7396

Downloaded from https://www.science.org at National University of Ireland, Galway on August 20, 2025